Bandwidth-tunable add–drop filters based on micro-electro-mechanical-system actuated silicon microtoroidal resonators

Jin Yao* and Ming C. Wu

Department of Electrical Engineering and Computer Sciences, University of California, Berkeley, Berkeley, California 94720, USA
**Corresponding author: jinyao@berkeley.edu*

Received May 20, 2009; revised July 27, 2009; accepted July 29, 2009;
posted August 3, 2009 (Doc. ID 111540); published August 19, 2009

A bandwidth-tunable filter has been demonstrated based on a micro-electro-mechanical-system (MEMS) actuated single-crystalline silicon microtoroidal resonator. Bandwidth is tuned from 2.8 to 78.4 GHz by voltage control, the largest bandwidth tuning range reported to date to our knowledge in resonator-based filters. A 21.8 dB extinction ratio is attained as a dynamic add–drop filter. © 2009 Optical Society of America
OCIS codes: 130.3120, 140.4780, 120.2440.

Tunable optical filters are key components in reconfigurable wavelength-division-multiplexing (WDM) networks. Wavelength-tunable filters can add, drop, switch, or block selected wavelength channels. Filters with tunable bandwidth are useful in dynamic bandwidth allocation for optimal spectral efficiency and in optical performance monitoring [1]. Bandwidth-tunable filters have been demonstrated using a micro-electro-mechanical-system (MEMS) micromirror-based Gires–Tournois interferometer [2] and mechanically stretched fiber Bragg gratings [3]. However, these filters are bulky and cannot be easily integrated.

Microresonators have been widely studied for various filtering functions [4,5]. Using a thermal tuning mechanism, an integrated bandwidth-tunable filter has been demonstrated at the through port with a tuning range of 12.5 GHz to 87.5 GHz (0.1 nm to 0.7 nm) around the wavelength of 1550 nm [6]. However, thermally tuned devices require continuous power to maintain the bandwidth. Using MEMS-actuated voltage-control mechanisms, bandwidth-tunable filters based on microdisk resonators have been reported, demonstrating a bandwidth tuning range around 1550 nm wavelength from 12 to 27 GHz at the through port [7]. With on-chip microheater integration, both wavelength and bandwidth tunability were achieved with a bandwidth tuning range from 12 to 41 GHz at the drop port [8]. System-level functions such as matched filtering, dynamic channel banding, and wavelength demultiplexing have also been demonstrated [9]. However, the lack of radial mode control in microdisk resonators limits the maximum tuning range owing to excitation of high-order modes. Here, we report on a reconfigurable and bandwidth-tunable add–drop filter with a large tuning range using a single-crystalline silicon microtoroidal resonator. Microtoroidal resonators offer tighter optical confinement and eliminate multiple radial modes observed in the microdisks. We have achieved a FWHM bandwidth tuning range of 2.8 GHzto 78.4 GHz. To our knowledge, this is the largest bandwidth tuning range in microresonator-based filters reported to date.

The tunable filter consists of a high-quality-factor (high-Q) silicon microtoroidal resonator, and input and output deformable waveguides, integrated in a two-layer silicon-on-insulator (SOI) structure, as shown in Fig. 1(a). The waveguides are suspended around the microtoroid. Upon electrostatic actuation, the waveguide is deformed and pulled toward the microtoroid, changing the power-coupling ratio. Figure 1(b) shows scanning electron microscope (SEM) images of a fabricated microtoroidal resonator. The resonator has a ring radius of 19.5 μm and a toroidal radius of 200 nm. This toroidal profile provides a tighter optical confinement than a microdisk does and allows for a single radial mode, as verified in the experimental results shown in Fig. 2. The waveguides are 0.69 μm wide and 0.25 μm thick. They are slightly multimode at the wavelength of 1.55 μm. The power is launched primarily into the fundamental mode. Details of the device integration design and fabrication process were reported elsewhere [10].

According to the time-domain coupling theory [4], the optical transmission is determined by the relationship between the resonator intrinsic loss and the power-coupling ratios of the input and output waveguides. For high-Q resonators, the losses are low, and the filter bandwidths are dominated by coupling. By controlling the coupling ratios, we can achieve the dynamic add–drop function and vary the bandwidth of the signal spectra.

A broadband amplified spontaneous emission (ASE) source is used to measure the spectral response of the through and drop ports. Owing to the group index difference, TE- and TM-polarized light has different resonances. Using a polarizer and a polarization controller, the input light is controlled to be TE polarized. Spherical lensed fibers with spot sizes of 2.5 μm are used as the input and output fi-

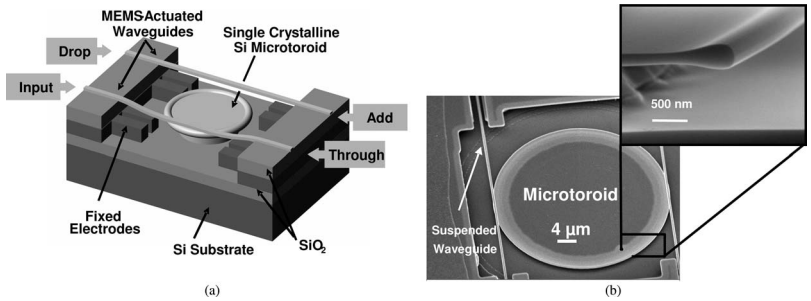

Fig. 1. (a) Schematic of the microtoroidal resonator tunable filter. (b) SEM of a fabricated microtoroidal resonator, with the inlet showing the toroid edge.

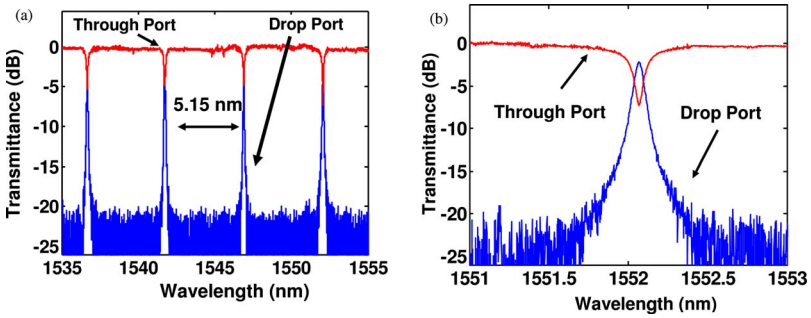

Fig. 2. (Color online) (a) Measured spectral response of the through and the drop port at actuation voltages of 32.8 V. (b) Detailed spectral response around the resonant wavelength of 1552.1 nm.

bers. For a practical filter, polarization-maintaining fiber can be used to ensure the incident polarization. If the input polarization is random, as in the case of a receiver, polarization diversity may be employed to mitigate the polarization dependence.

With a zero voltage bias, the input power is transmitted to the through port with negligible coupling to the drop port. When the electrostatic actuators are biased, the optical powers at resonant wavelengths decrease at the through port as they are transferred to the drop port. Figure 2 shows the spectral response of the through and the drop ports at biases of 32.8 V. The measured free spectral range (FSR) is 5.15 nm. Figure 3 shows the transmittance versus the applied voltages for both the through and the drop ports at a resonant wavelength of 1552.1 nm. A 21.8 dB extinction ratio is measured when the voltages are changed from 0 V to 58.1 V for both waveguides. This device can be used as a dynamic add–drop filter. The extinction ratio can be further improved by controlling the voltages to change the power-coupling ratio of the input and output waveguides, to achieve theoretical zero output of the through port, as indicated in Eq. (1) below.

To demonstrate bandwidth tunability, we control the bias of each waveguide separately and measure the FWHM bandwidth of the drop port. Figure 4 shows the transmission spectra of the drop port for various power-coupling ratios at a resonant wavelength of 1552.1 nm. When the bias voltages of input and drop waveguides are 32.7 V and 35.9 V, respectively, the FWHM bandwidth is 2.8 GHz, as shown by curve (a) in Fig. 4. As the actuation voltages increase, the power-coupling ratios also increase, which leads to larger bandwidth, as shown by curves (b) through (g). With 48.6 V (input port) and 58.1 V (drop port), the bandwidth increases to 78.4 GHz, as shown by curve (g).

According to the time-domain coupling theory [4,7], the optical transmission can be expressed as a function of resonant frequency (ω_0), power-coupling ratios of the input and output waveguides (κ_1 and κ_2, respectively), round-trip propagation time (T_R), and round-trip resonator loss (γ),

$$T_{\text{through}}(\omega) = \frac{j(\omega-\omega_0)+(\gamma+\kappa_2-\kappa_1)/2T_R}{j(\omega-\omega_0)+(\gamma+\kappa_2+\kappa_1)/2T_R}, \qquad (1)$$

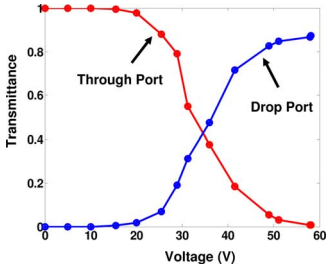

Fig. 3. (Color online) Measured transmittance versus actuation voltages at the resonant wavelength of 1552.1 nm.

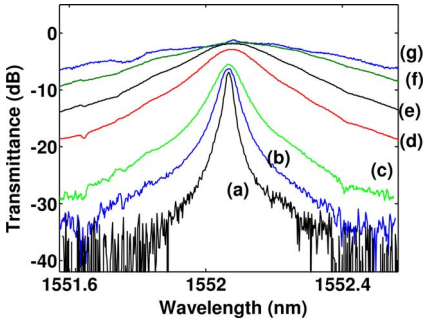

Fig. 4. (Color online) Measured spectral response at the drop port for several actuation biases.

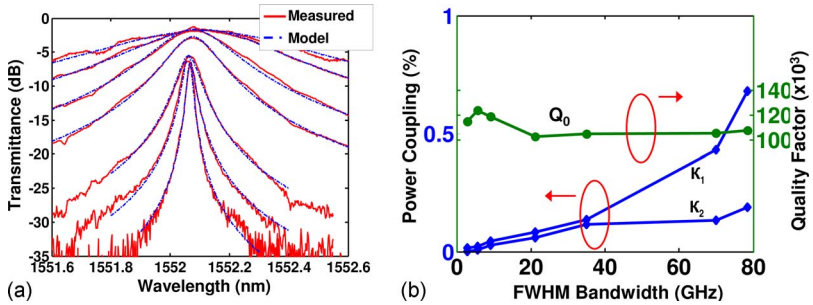

Fig. 5. (Color online) (a) Measured and modeled spectra at the drop port with the bias conditions the same as in Fig. 4. (b) Calculated unloaded Q and the power-coupling ratios versus the FWHM bandwidth of the spectra.

$$T_{\text{drop}}(\omega) = \frac{\sqrt{\kappa_1\kappa_2}/T_{\text{R}}}{j(\omega-\omega_0)+(\gamma+\kappa_2+\kappa_1)/2T_{\text{R}}}, \qquad (2)$$

where $T_{\text{through}}(\omega)$ and $T_{\text{drop}}(\omega)$ represent the amplitude transfer functions at the through and drop ports, respectively, and $\gamma = 4\pi^2 R \cdot n_g/Q_0\lambda_0$, where n_g is the effective group index of the mode, R is the radius of the microresonator, Q_0 is the unloaded quality factor, and λ_0 is the resonant wavelength.

Using this model, the unloaded quality factors, Q_0, and the power-coupling ratio, κ_1 and κ_2, are extracted from the measured optical spectra by least-mean-square-error fitting to the model. Figure 5(a) shows the measured and fitted spectra around the resonance peak at 1552.1 nm when the filter bandwidth is tuned corresponding to curves (a) through (g) in Fig. 4. The experimental spectra matched very well with the theoretical model. From the fitted spectral response, the unloaded quality factor, Q_0, of the microtoroidal resonator is extracted to be around 110,000. The power-coupling ratio κ_1 increases from 1.6% to 67%, and κ_2 from 0.2% to 19%, when the FWHM bandwidth is tuned from 2.8 GHz to 78.4 GHz, as shown in Fig. 5(b).

When κ_1 and κ_2 are much larger than γ ($\kappa_1, \kappa_2 \gg \gamma$), the filter is operated in the strongly overcoupled regime. At the drop port, the insertion loss at the resonant wavelength can be very small, as Eq. (2) indicated,

$$T_{\text{drop}}(\omega_0) = \frac{\sqrt{\kappa_1\kappa_2}/T}{(\gamma+\kappa_2+\kappa_1)/2T} \approx \frac{\sqrt{\kappa_1\kappa_2}}{(\kappa_2+\kappa_1)/2} \le 1. \qquad (3)$$

This permits the bandwidth tuning while maintaining a low insertion loss. As shown in Fig. 5, the lowest insertion loss demonstrated is −1.5 dB with FWHM of 78.4 GHz, when κ_1 and κ_2 are 67% and 19%, respectively. When κ_1 and κ_2 are controlled to approach γ and to move toward slightly overcoupled regimes, the insertion loss at the resonant wavelength starts to increase, as shown in the spectra with narrower bandwidths in Fig. 4. This indicates that, since γ is inversely proportional to Q_0, a high-Q microresonator is beneficial and desired for bandwidth tuning applications to achieve low loss and large tuning range simultaneously.

In conclusion, we have demonstrated a monolithically integrated dynamic add–drop filter with tunable bandwidth using the MEMS-actuated single-crystalline silicon microtoroidal resonator. The FWHM bandwidth is continuously tunable from 2.8 GHz to 78.4 GHz. To the authors' best knowledge, this is the largest bandwidth tuning range in microresonator-based filters reported to date. Using the time domain coupling theory, a theoretical model is established. The experimental and theoretical results agreed very well. From the fitted spectral response, the unloaded quality factor of the microtoroidal resonator is extracted to be 110,000. The power-coupling ratio κ_1 increases from 1.6% to 67%, and κ_2 from 0.2% to 19%. As a dynamic add–drop filter, wavelength switching with a 21.8 dB extinction ratio is attained. These types of tunable filters have potential applications in dynamic bandwidth allocation, optical performance monitoring, signal processing, and sensing.

The authors acknowledge support from the National Science Foundation (NSF) through the Engineering Research Center for Integrated Access Networks (ERC CIAN) under grant EEC-0812072.

References

1. Q. Yu, Z. Pan, L.-S. Yan, and A. E. Willner, J. Lightwave Technol. **20**, 2267 (2002).
2. K. Yu and O. Solgaard, IEEE J. Sel. Top. Quantum Electron. **10**, 588 (2004).
3. X. Dong, P. Shum, N. Q. Ngo, C. Zhao, J. Yang, and C. C. Chan, Microwave Opt. Technol. Lett. **41**, 22 (2004).
4. B. E. Little, S. T. Chu, H. A. Haus, J. Foresi, and J. P. Laine, J. Lightwave Technol. **15**, 998 (1997).
5. D. Rafizadeh, J. P. Zhang, S. C. Hagness, A. Taflove, K. A. Stair, S. T. Ho, and R. C. Tiberio, Opt. Lett. **22**, 1244 (1997).
6. L. Chen, N. Sherwood-Droz, and M. Lipson, Opt. Lett. **32**, 3361 (2007).
7. M. C. Lee and M. C. Wu, Opt. Lett. **31**, 2444 (2006).
8. J. Yao, M.-C. M. Lee, D. Leuenberger, and M. C. Wu, paper presented at the 2006 Optical Fiber Communication Conference and National Fiber Optic Engineers Conference, Anaheim, California, 5–10 March 2006.
9. B. Zhang, D. Leuenberger, M.-C. M. Lee, A. E. Willner, and M. C. Wu, IEEE Photonics Tech. Lett. **19**, 1508 (2007).
10. J. Yao, D. Leuenberger, M.-C. M. Lee, and M. C. Wu, IEEE J. Sel. Top. Quantum Electron. **13**, 202 (2007).